Journal of Veterinary Cardiology (2019) **23**, 104—111

Journal of Veterinary Cardiology
ESVC

www.elsevier.com/locate/jvc

Case Report

Transcatheter embolization of systemic-to-pulmonary artery fistulas in a dog using embolization coils and silk suture☆,☆☆

R.L. Winter, DVM[a,*], J.A. Horton, MD[b], D.K. Newhard, DVM[c], M. Holland, DVM, MS[c]

[a] *Department of Veterinary Clinical Sciences, The Ohio State University College of Veterinary Medicine, 601 Vernon L. Tharp St, Columbus, OH, 43210, USA*
[b] *Department of Medicine, Tulane University School of Medicine, 131 South Robertson Avenue, New Orleans, LA, 70112, USA*
[c] *Department of Small Animal Clinical Sciences, College of Veterinary Medicine and Biomedical Sciences, Auburn University, 1220 Wire Road, Auburn, AL, 36849, USA*

Received 23 July 2018; received in revised form 28 January 2019; accepted 21 February 2019

KEYWORDS
Canine;
Congenital heart disease;
Interventional;

Abstract A 4-month-old intact female Cavalier King Charles spaniel presented for evaluation of a left, basilar continuous murmur. Transthoracic echocardiography suggested anomalous vessels around the main pulmonary artery, and computed tomography angiography revealed two systemic-to-pulmonary artery fistulas. Transcatheter embolization of these fistulas was achieved with a

Abbreviations: AVF, arteriovenous fistula; CTA, computed tomography angiography; LPA, left pulmonary artery; SPAF, systemic-to-pulmonary artery fistula.

☆ A unique aspect of the Journal of Veterinary Cardiology is the emphasis of additional web-based images permitting the detailing of procedures and diagnostics. These images can be viewed (by those readers with subscription access) by going to http://www.sciencedirect.com/science/journal/17602734. The issue to be viewed is clicked and the available PDF and image downloading is available via the Summary Plus link. The supplementary material for a given article appears at the end of the page. Downloading the videos may take several minutes. Readers will require at least Quicktime 7 (available free at http://www.apple.com/quicktime/download/) to enjoy the content. Another means to view the material is to go to http://www.doi.org and enter the doi number unique to this paper which is indicated at the end of the manuscript.

☆☆ A unique aspect of the Journal of Veterinary Cardiology is the emphasis of additional web-based materials permitting the detailing of procedures and diagnostics. These materials can be viewed (by those readers with subscription access) by going to http://www.sciencedirect.com/science/journal/17602734. The issue to be viewed is clicked and the available PDF and image downloading is available via the Summary Plus link. The supplementary material for a given article appears at the end of the page. To view the material is to go to http://www.doi.org and enter the doi number unique to this paper which is indicated at the end of the manuscript.

* Corresponding author.
E-mail address: winter.159@osu.edu (R.L. Winter).

https://doi.org/10.1016/j.jvc.2019.02.003
1760-2734/© 2019 Elsevier B.V. All rights reserved.

Vascular;
Occlusion

combination of embolization coils and silk suture threads delivered through a microcatheter.
© 2019 Elsevier B.V. All rights reserved.

A 4-month-old, 4-kg, intact female Cavalier King Charles spaniel was referred to the Auburn University Veterinary Teaching Hospital for evaluation of a continuous heart murmur. The dog had no clinical signs attributable to cardiovascular disease, and the heart murmur was detected during a routine examination with the primary care veterinarian. Physical examination confirmed a grade II/VI left basilar systolic heart murmur. Hyperdynamic femoral arterial pulses were also detected. Thoracic radiographs disclosed mild left atrial enlargement with a vertebral heart size of 10.0 (normal $\leq$ 10.5) [1]. Transthoracic echocardiographic findings included subjectively normal right atrial and right ventricular size. Left ventricular internal dimensions in systole and in diastole were normal [2]. There was a mild increase in the left atrial size, with a left atrial to aortic root ratio of 1.7 [3]. Trivial pulmonic insufficiency was present. Color Doppler interrogation revealed multiple areas of turbulent blood flow near the bifurcation of the main pulmonary artery, some of which were observed flowing into the left pulmonary artery (LPA) during diastole (Fig. 1A).

Further diagnostics included a complete blood count and a serum biochemistry panel, both of which revealed no significant laboratory abnormalities. Transesophageal echocardiography, selective angiography, and precontrast and postcontrast computed tomography angiography[c] (CTA) were scheduled for the following day.

After anesthetic induction, the dog was placed in right lateral recumbency. Transesophageal echocardiography was challenging due to patient size, but it revealed continuous turbulent blood flowing into the proximal LPA (Fig. 1B). Based on the location of the turbulent blood flow entering the LPA near its origin, the authors' considered a patent ductus arteriosus or similar vessel a possibility and therefore entered the femoral artery for selective angiography. The right femoral artery was exposed via surgical cutdown, and arterial access was obtained with a 6-Fr introducer[d] using the modified Seldinger approach. A 4-Fr guiding catheter[e] was advanced through the vascular introducer to the level of the proximal descending aorta. Selective angiography revealed a tortuous, anomalous vessel originating from the brachiocephalic trunk that terminated at the LPA (Fig. 2A, Supplemental Video I). The introducer was removed, and the femoral artery was ligated without complication. Contrast-enhanced CTA was performed using 64-slice scanner with a solid-state array using a 40-mm detector size collimator. The precontrast scan was performed in 5.0-mm—slice thickness from the thoracic inlet to the cranial abdomen to the level of the 12th rib. Acquisition of the postcontrast images was obtained after initiation of the hand-injected dose of 10-ml contrast. The postcontrast images had three sequential timed sequences initiated during administration of the contrast dose. Each sequence had an exposure time of 5.6 s with a 2.0 s delay between the sequences. Each of the three sequences had adequate contrast attenuation present in the cardiovascular system. The postcontrast images were reconstructed in 0.625-mm—thickness before volume rendering for the vascular models. The CTA revealed two anomalous systemic-to-pulmonary artery fistulas (SPAFs), both of which terminated in the LPA (Fig. 2C). One of these fistulas originated from the brachiocephalic trunk, and the other anomalous vessel originated between the origins of the left and right common carotid arteries. The dog recovered uneventfully from anesthesia and was sent home the following day. Owing to the presence of left atrial enlargement and concern of future left heart volume overload from myxomatous mitral valve disease, the owner elected to pursue transcatheter embolization.

Four weeks later, the dog was returned for transcatheter embolization. After anesthetic induction, the dog was placed in left lateral recumbency. The left femoral artery was exposed

[c] GE Lightspeed VCT, Milwaukee, WI, USA.
[d] 6Fr Introducer, Boston Scientific, Natick, MN, USA.
[e] 4Fr Flexor Check Flo catheter®, COOK® Medical, Bloomington, IN, USA.

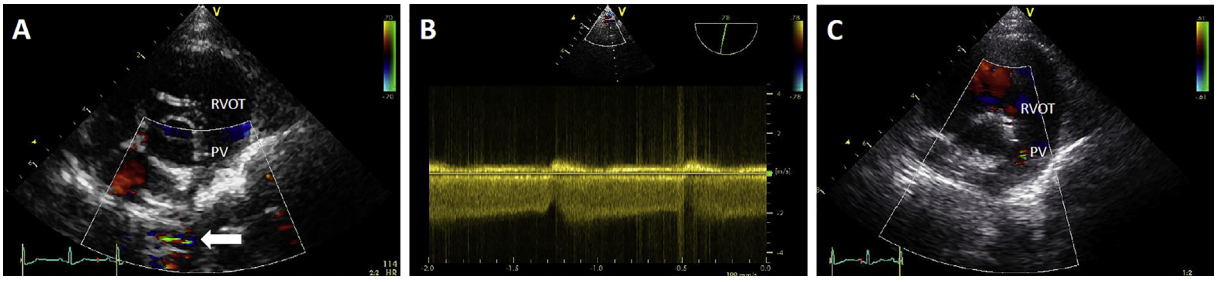

Fig. 1 (A) Preprocedural TTE right parasternal short-axis view highlighting multiple, abnormal blood flow signals (arrow) observed near the bifurcation of the main pulmonary artery. (B) Continuous, turbulent blood flow documented entering the LPA with TEE while the dog was anesthetized. (C) TTE right parasternal short-axis view obtained 1 day postoperatively, highlighting the absence of the abnormal blood flow signals previously observed. LPA, left pulmonary artery; PV, pulmonic valve; RVOT, right ventricular outflow tract; TEE, transesophageal echocardiography; TTE, transthoracic echocardiography.

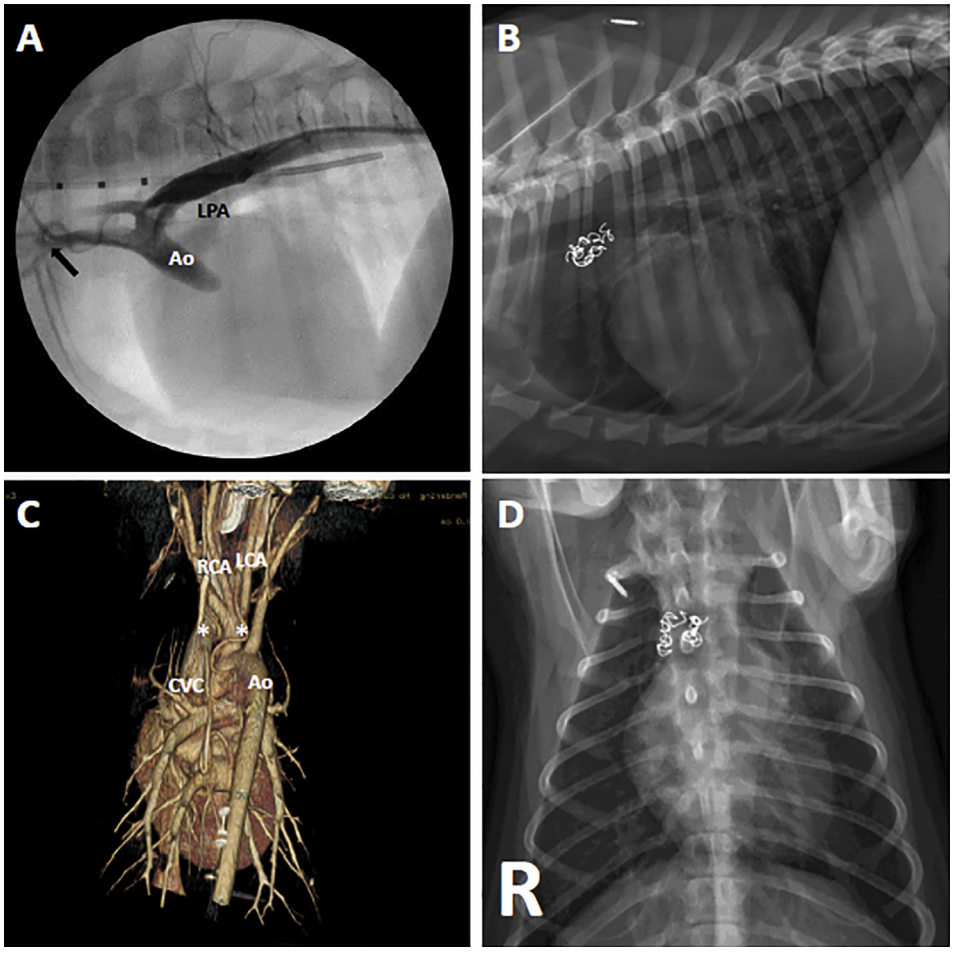

Fig. 2 (A) Preprocedural right lateral angiogram of the descending aorta demonstrating the origin from the brachiocephalic trunk (arrow) and the termination in the LPA of a SPAF. (B) Postprocedural right lateral thoracic radiograph demonstrating the embolization coils within two SPAFs. (C) Three-dimensional volume-rendered image of the heart and associated vessels demonstrating the presence of two SPAFs* and the origin of one SPAF between the LCA and RCA. (D) Postprocedural ventrodorsal thoracic radiograph demonstrating the embolization coils within the two SPAFs. Ao, aorta; CVC, cranial vena cava; LCA, left common carotid artery; LPA, left pulmonary artery; RCA, right common carotid artery; SPAF, systemic-to-pulmonary artery fistulas.

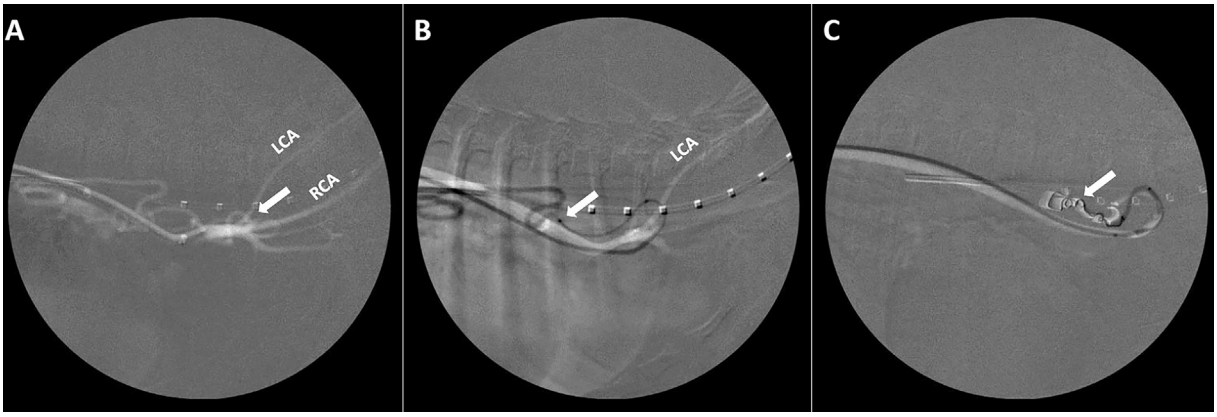

Fig. 3 (A) Left lateral angiographic view obtained by rotating the image intensifier 60° toward the spine without changing cranial/caudal angulation demonstrating the origin of one SPAF (arrow) between the origins of the LCA and RCA. (B) Obliqued left lateral angiographic view demonstrating the location of the microcatheter (arrow) within one SPAF for selective angiography. (C) Obliqued left lateral angiographic view demonstrating a lack of contrast flow past the deployed combination of embolization coil (arrow) and silk suture thread within one SPAF. LCA, left common carotid artery; RCA, right common carotid artery; SPAF, systemic-to-pulmonary artery fistula.

via surgical cutdown, and arterial access was obtained with a 4-Fr introducer[f] using the modified Seldinger approach. A 4-Fr non-taper angled 100-cm length catheter[g] over a 0.018 × 180 cm hydrophilic guidewire[h] was advanced into the brachiocephalic trunk. Multiple contrast injections were performed to identify the origin of these fistulas. In addition, the C-arm was manipulated to create several different obliqued views, until satisfactory visualization of the fistula origin was achieved by rotating the image intensifier 60° toward the spine without changing cranial/caudal angulation. The 4-Fr non-taper angled catheter was advanced to the origin of the fistula as the base catheter, and then, a 2.8-Fr microcatheter[i] was advanced through the base catheter into the fistula using road mapping for navigation (Fig. 3A and B, Supplemental Video II). Selective microcatheter angiography confirmed the position.

Once the microcatheter was advanced roughly 5 cm into the fistula, a 0.018″ × 3 mm × 7 cm embolization coil[j] was deployed into the fistula. After waiting for roughly 10 min, selective angiography of the fistula revealed residual flow past the coil into the LPA. We then injected a 1-inch long segment of 3-0 silk suture[k] through the microcatheter into the fistula at the level of the coil. This was achieved by placing the silk suture segment into the distal segment of a 20 g IV catheter and then securing that IV catheter to a 3-mL luer-lock syringe filled with 3 mL of heparinized saline. The tip of the IV catheter was then pushed into the hub of the microcatheter before steady, controlled injection. Selective angiography then revealed no residual flow past the coil (Fig. 3C). The same approach was then used to enter the second fistula with the microcatheter (Fig. 4A, Supplemental Video III). A 0.018" × 3 mm × 7 cm embolization coil[j] was then deployed into this fistula. Similarly, mild residual flow past the embolization coil was observed 10 min after deployment (Fig. 4B). Again, a 1-inch length segment of 3-0 silk suture was injected into the second fistula at the level of the embolization coil, and no residual flow past the coil was observed immediately afterward (Fig. 4C, Supplemental Video IV). The introducer was removed, and the femoral artery was ligated. The total procedure time was 2 h 30 min, and the dog recovered uneventfully.

Thoracic radiographs performed the following day confirmed coil placement. The lack of the previously identified abnormal blood flow near and into the LPA artery was confirmed with transthoracic echocardiography (Fig. 1C). Cardiac auscultation revealed no heart murmur. The dog had no pain associated with the rear limbs and had normal ambulation. A repeat serum biochemistry revealed

[f] 4Fr Check Flo Introducer®, COOK® Medical, Bloomington, IN, USA.
[g] 4Fr Non-taper Angle catheter, Terumo Medical, Somerset, NJ, USA.
[h] Radiofocus® hydrophilic coated guidewire, Terumo Medical, Somerset, NJ, USA.
[i] PROGREAT® 2.8Fr Microcatheter, Terumo Medical, Somerset, NJ, USA.
[j] Nester® Platinum Embolization Microcoils, COOK® Medical, Bloomington, IN, USA.
[k] 3—0 Perma-hand Silk suture, Ethicon, Athens, GA, USA.

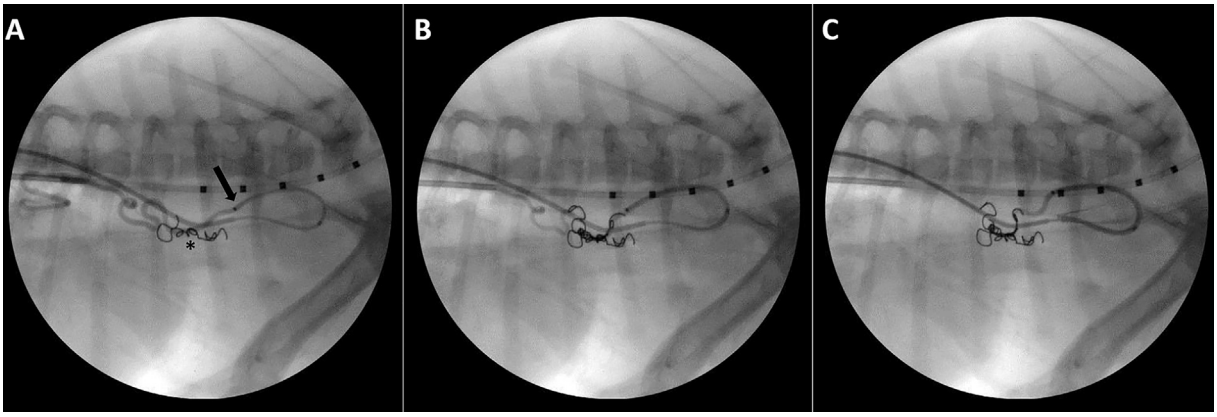

Fig. 4 (A) Left lateral angiographic view obtained by rotating the image intensifier 60° toward the spine without changing cranial/caudal angulation demonstrating the location of the microcatheter (arrow) within the second SPAF for selective angiography after embolization of the first SPAF with an embolization coil* and silk suture thread. (B) Obliqued left lateral angiographic view demonstrating residual flow past the deployed embolization coil within the second SPAF. (C) Obliqued left lateral angiographic view demonstrating no residual flow past the deployed combination of embolization coil and silk suture thread within the second SPAF. SPAF, systemic-to-pulmonary artery fistula.

no abnormalities. Two months after the procedure, the dog was presented for a scheduled recheck. Abnormal blood flow was observed entering the LPA on transthoracic echocardiography, which was judged to be trivial based on the minimal size (width and length of extension into the main pulmonary artery) of the jet of color flow. Based on the location of entry into the main pulmonary artery, the authors speculate that this could represent recanalization of the treated fistula/s. The vertebral heart size had decreased and was 9.2, and the left atrium was decreased in size compared with the previous examination with a left atrial to aortic root ratio of 1.1 [3]. All other findings were unchanged compared with the previous echocardiographic examination. Thoracic radiography revealed that the embolization coils had not migrated (Fig. 2B and D). Cardiac auscultation still revealed no heart murmur. The dog ambulated normally and had no pain associated with the rear limbs.

Discussion

In the dog, arteriovenous fistulas (AVFs) and similar lesions have been reported relatively uncommonly [4—8]. Anatomic locations of AVF in the dog include central locations such as systemic-to-pulmonary connections and abdominal aortocaval connections, to more peripheral locations such as the saphenous artery [4—7,9]. These abnormal vascular connections range in size from small enough to be occluded with a single embolization coil [5,7] to extensive lesions sometimes requiring staged procedures [6,10,11]. Many of these AVFs are congenital in origin like the dog in this report, although some are considered as acquired secondary to diseases such as trauma [7,8,12,13]. The dog in this report had two SPAFs, which were likely congenital in origin based on their morphology. Both AVF and SPAF may induce volume overload to the pulmonary arteries and veins. Systemic-to-pulmonary artery fistulas may have similar presenting clinical signs as the more commonly diagnosed disease patent ductus arteriosus, namely a continuous heart murmur and evidence of left heart enlargement or pulmonary overcirculation [4,6,14]. Selective angiography and CTA are commonly used for both definitive diagnosis and for treatment planning. In the dog in this report, selective aortic angiography revealed the presence of one fistula, highlighting its origin from the lateral aspect of the brachiocephalic trunk and its termination in the LPA. However, CTA was essential to identify the full number and extent of both fistulas in this dog.

There are several factors to consider when deciding whether an interventional procedure is warranted for AVF or other anomalous vessels like the ones described in this report. Shunting of blood into the pulmonary circulation can cause pulmonary overcirculation, which may be detected radiographically or echocardiographically, and this can lead to left heart enlargement [6,10,14,15]. In addition, chronic pulmonary overcirculation may lead to severe pulmonary arterial remodeling, resulting in pulmonary hypertension [9,16]. The dog in this report had no evidence of pulmonary hypertension and no obvious signs of pulmonary overcirculation. The left atrium was enlarged when compared with an adult-derived reference range [3], and the

appearance of the left atrium was subjectively enlarged. The presence of left atrial enlargement, hyperdynamic femoral arterial pulse, and the size of the fistulas suggested these to be hemodynamically important shunts. The overall heart size was normal, and there was no obvious pulmonary overcirculation, which would suggest it was not necessary to embolize these fistulas. Weighing these factors plus considering the breed of this dog and the likelihood of future left heart volume overload due to myxomatous mitral valve disease, the owner elected to pursue embolization before any further cardiovascular remodeling might occur. The decrease in the left atrial size after embolization suggests the shunts were hemodynamically significant.

Embolization techniques are used either alone or in combination in humans with AVF and other anomalous vessels include embolization coils, vascular occlusion devices such as vascular plugs, polyvinyl alcohol particles and other liquid embolic agents, and silk suture [17—20]. In dogs, anomalous vessels have been embolized with embolization coils [5—7], vascular occlusion devices [21,22], and liquid embolic agents including polyvinyl alcohol particles and n-butyl cyanoacrylate [10,11,23,24]. Vascular occlusion devices are limited in use to those vessels large enough to accommodate them. Embolization coils can be deployed into very small vessels, and platinum 0.018" coils can be delivered through microcatheters as in the dog in this report. The liquid embolic agents, polyvinyl alcohol particles, n-butyl cyanoacrylate, and ethylene—vinyl alcohol copolymer, were all inappropriate in this case owing to the risk of particulate emboli traversing the shunts to enter the pulmonary artery [17]. In both humans and dogs, the decision as to what material to use is based on the nature of the lesion (i.e. large vs. small vascular structures) and operator experience. In the dog in this report, a combination of embolization coils and silk suture threads was used to embolize the fistulas. Immediate, complete embolization was observed, but a trivial amount of flow had returned at the recheck. Further examinations will determine if additional action is required.

Silk suture threads for embolization have been used in humans to occlude renal arteriovenous malformations [20], seal coronary artery perforations [19], and occlude cerebral arteriovenous malformations [18,25,26]. Studies evaluating silk suture as an embolic agent found it to be safe with rare instances of perivascular inflammation and hemorrhage [25,26]. In addition, silk suture is inexpensive and often readily available. The authors chose to inject silk suture threads to aid in complete fistula occlusion, which decreased anesthetic time. Once silk is injected into a vessel, a rapid local thrombogenesis occurs. In the dog of this case, residual flow past the coil was still present 10 min after placement. Although more time may have allowed the fistulas to be occluded with an embolization coil alone, this would have required additionally time to wait while the patient was anesthetized. The addition of more embolization coils was deemed dangerous based on the size of these fistulas, specifically that they might not have fit and thus prolapsed back into the parent artery. In addition, adding more coils would have been a more costly option. By deploying the embolization coils first, the silk suture was provided a scaffold to attach to once injected. Although silk suture is radiolucent, the near-instantaneous thrombosis proved correct deployment location.

In conclusion, we describe a case of transcatheter embolization of SPAF in a dog using a combination of embolization coils and silk suture. Excellent visualization of the fistulas was achieved using CTA, optimally obliqued fluoroscopic angles and road mapping angiography. Embolization of the fistulas was achieved with a combination of embolization coils and silk suture, which to the authors' knowledge has not been previously reported in the dog. The injection of silk suture threads into an anomalous vessel partially occluded with embolization coils may be a safe, expedient, and effective way to approach embolization in similar cases.

Conflict of interest statement

The authors have no conflict of interest.

Acknowledgments

The authors thank Silas Zee for his assistance with generation of figures and videos for the manuscript.

Supplementary data

Supplementary data to this article can be found online at https://doi.org/10.1016/j.jvc.2019.02.003.

Video table

Video	Title	Description
I	Initial descending aortic angiogram	Injection into the descending aorta demonstrates a fistula originating from the brachiocephalic trunk and terminating into the left pulmonary artery.
II	Initial selective angiogram into the first fistula	Entry into the first fistula by the microcatheter is observed, and a selective angiogram demonstrates its tortuous route before termination into the left pulmonary artery. The view is an obliqued left lateral view.
III	Initial selective angiogram into the second fistula	Entry into the second fistula by the microcatheter is observed, and a selective angiogram demonstrates its tortuous route before termination into the left pulmonary artery. The view is an obliqued left lateral view. The presence of the embolization coil in the first fistula is observed.
IV	Final selective angiogram into the second fistula	After the embolization coil and silk suture thread have been deployed into the second fistula, a final selective angiogram demonstrates lack of residual flow past the combined embolization coil and silk suture thread. Increased pressure from distal occlusion within the fistula causes back flow of contrast at the proximal origin of this fistula.

References

[1] Buchanan JW, Bucheler J. Vertebral scale system to measure canine heart size in radiographs. J Am Vet Med Assoc 1995;206:194—9.

[2] Cornell CC, Kittleson MD, Della Torre P, Haggstrom J, Lombard CW, Pederson HD, Vollmar A, Wey A. Allometric scaling of M-mode cardiac measurements in normal adult dogs. J Vet Intern Med 2004;18:311—21.

[3] Rishniw M, Erb HN. Evaluation of four 2-dimensional echocardiographic methods of assessing left atrial size in dogs. J Vet Intern Med 2000;14:429—35.

[4] Newhard DK, Winter RL, Cline KA, Hathcock JT. Anomalous broncho-oesophageal arteries and peripheral systemic-to-pulmonary connections in an asymptomatic puppy. Vet Rec Case Rep 2017;5:e000392.

[5] Nakata TM, Tanaka R, Hamabe L, Yoshiyuki R, Kim S, Suzuki S, Aytemiz D, Huai-Che H, Shimizu M, Fukushima R. Transarterial coil embolization of an abdominal aortocaval fistula in a dog. J Vet Intern Med 2014;28:656—60.

[6] Leach SB, Fine DM, Schutrumpf RJ, Britt LG, Durham HE, Christiansen K. Coil embolization of an aorticopulmonary fistula in a dog. J Vet Cardiol 2010;12:211—6.

[7] Saunders AB, Fabrick C, Achen SE, Miller MW. Coil embolization of a congenital arteriovenous fistula of the saphenous artery in a dog. J Vet Intern Med 2009;23:662—4.

[8] Cocca CJ, Weisse C, Berent AC, Rosen R. Minimally invasive treatment of mesenteric arterioportal fistulas in two dogs. J Am Vet Med Assoc 2017;251:1306—12.

[9] Ledda G, Caldin M, Mezzalira G, Bertolini G. Multidetector-row computed tomography patterns of bronchoesophageal artery hypertrophy and systemic-to-pulmonary fistula in dogs. Vet Radiol Ultrasound 2015;56:347—58.

[10] Eason BD, Hogan DF, Lim C, Hogan MJ. Use of n-butyl cyanoacrylate to reduce left to right shunting of an abdominal arteriovenous malformation in a dog. J Vet Cardiol 2017;19:396—403.

[11] Case JB, Boston SE, Porter EP, Toskich BB. Endovascular treatment of a high-flow hepatic arteriovenous malformation with secondary portal hypertension in a dog. J Am Vet Med Assoc 2017;251:824—8.

[12] Santoro D, Pease A, Linder KE, Olivry T. Post-traumatic peripheral arteriovenous fistula manifesting as digital haemorrhages in a cat: diagnosis with contrast-enhanced 3D CT imaging. Vet Dermatol 2009;20:206—13.

[13] Aiken SW, Jakovljevic S, Lantz GC, Blevins WE. Acquired arteriovenous fistula secondary to castration in a dog. J Am Vet Med Assoc 1993;202:965—7.

[14] Fujii Y, Aoki T, Takano H, Ishikawa R, Wakao Y. Arteriovenous shunts resembling patent ductus arteriosus in dogs: 3 cases. J Vet Cardiol 2009;11:147—51.

[15] Serres F, Chetboul V, Tissier R, Gouni V, Desmyter A, Sampedrano CC, Pouchelon J-L. Quantification of pulmonary to systemic flow ratio by a Doppler echocardiographic method in the normal dog: repeatability, reproducibility, and reference ranges. J Vet Cardiol 2009;11:23—9.

[16] Heath D, Donald DE, Edwards JE. Pulmonary vascular changes in a dog after aortopulmonary anastomosis for four years. Br Heart J 1959;21:187—96.

[17] Vaidya S, Tozer KR, Chen J. An overview of embolic agents. Semin Intervent Radiol 2008;25:204—15.

[18] Conger JR, Ding D, Raper DM, Starke RM, Durst CR, Liu KC, Jensen ME, Evans AJ. Preoperative embolization of cerebral arteriovenous malformations with silk suture and particles: technical considerations and outcomes. J Cerebrovasc Endovasc Neurosurg 2016;18:90—9.

[19] Li Y, Wang G, Sheng L, Xue J, Sun D, Gong Y. Silk suture embolization for sealing distal coronary artery perforation: report of two cases. Rev Cardiovasc Med 2015;16:165—9.

[20] Gralino BJ, Bricker DL. Staged endovascular occlusion of giant idiopathic renal arteriovenous fistula with platinum microcoils and silk suture threads. J Vasc Intervent Radiol 2002;13:747—52.

[21] Weisse C, Mondschein JI, Itkin M, Iyoob C, Solomon JA. Use of a percutaneous atrial septal occluder device for complete acute occlusion of an intrahepatic portosystemic shunt in a dog. J Am Vet Med Assoc 2005;227:249—52.

[22] Hogan DF, Benitez ME, Parnell NK, Green 3rd HW, Sederquist K. Intravascular occlusion for the correction of extrahepatic portosystemic shunts in dogs. J Vet Intern Med 2010;24:1048—54.

[23] Weisse C, Clifford CA, Holt D, Solomon JA. Percutaneous arterial embolization and chemoembolization for treatment of benign and malignant tumors in three dogs and a goat. J Am Vet Med Assoc 2002;221:1430—6.

[24] Culp WTN, Glaiberman CB, Pollard RE, Wisner ER. Use of ethylene-vinyl alcohol copolymer as a liquid embolic agent to treat a peripheral arteriovenous malformation in a dog. J Am Vet Med Assoc 2014;245:216—21.

[25] Ding D, Sheehan JP, Starke RM, Durst CR, Raper DM. Embolization of cerebral arteriovenous malformations with silk suture particles prior to stereotactic radiosurgery. J Clin Neurosci 2015;22:1643—9.

[26] Schmutz F, McAuliffe W, Anderson DM, Elliott JP, Eskridge JM, Winn HR. Embolization of cerebral arteriovenous malformations with silk: histopathologic changes and hemorrhagic complications. Am J Neuroradiol 1997;18:1233—7.

Available online at www.sciencedirect.com

ScienceDirect